

EXPERIMENTAL INVESTIGATION OF CREEP BEHAVIOUR OF SATURATED SOFT CLAY SUBJECTED STATIC LOADING

*Ngoc Thang Nguyen¹

¹Civil and Industrial Construction Division, Faculty of Civil Engineering, Thuyloi University, Vietnam

*Corresponding Author, Received: 29 March 2023, Revised: 09 April 2023, Accepted: 23 April 2023

ABSTRACT: Creep of clayey soils is defined as the time-dependent deformation under sustained stresses, due to viscous behavior of the soil skeletons. The creep behavior of soil is influenced by several main factors, such as time, temperature, soil type, soil structure, stress history, stress state, and drainage conditions. Soft foundations of low embankments exhibit significant time-dependent effect on deformation in decades after construction, and there is a lack of simple method for predicting the creep rate of over-consolidated soft clay under plain strain condition. In this study, plane strain triaxial test have been conducted to investigation volumetric, axial and lateral creep strain of saturated soft clay. The experimental results show that the volumetric creep strain of soil specimens subjected to static loading increases with the increasing magnitude of external load, and it depends on the amplitude of pre-consolidation load, a larger pre-consolidation load value is associated with a significantly reduced volumetric creep strain. The variation of axial strain and lateral strain are similar with variation of volumetric creep strain for both normally and over-consolidated state, but the rate of variation decreases significantly when the soil transitions into an over-consolidated state. In addition, the test results show that the excess pore pressure develops and increases rapidly to reach the peak values as soon as the external loads was applied on the specimen and then decreases gradually to a stable value of zero during creep deformation stage of soil.

Keywords: Clay, Creep strain, Normally consolidated, Over-consolidated, Static loading

1. INTRODUCTION

The time-dependent deformation of cohesive soils results from both hydrodynamic lag (consolidation) and the viscous behavior of the soil skeleton (creep). The time-dependent behavior known as creep occurs in all soils, but the amount of creep differs depending on the soil type, its density, and the state of applied stress. Observations indicate that creep behavior is similar in principle for all types of soil. Because clays exhibit more creep deformation at given stress states than sands, clay soils have most often been the subject of studies of time-dependent behavior of soils [1, 2]. It has been established that preloading of clay is an effective means to reduce creep of the soil under working load conditions. After an initial rebound during unloading, a long-term viscous response occurs involving both creep and swelling [3].

The creep deformation of over consolidated soft soil is the main component of post-construction settlement of soft soil foundation and should not be ignored. It is considered as a truth that creep settlements of soft clay after primary consolidation are smaller than primary consolidation settlements. But, creep settlements of soft clay may affect the safe running of some civil engineering structures and had been a significant design issue, especially when the

structure is sensitive to its foundation ground movements or is lying on a very thick layer of soft clay [4]. The effect of creep deformation on subgrade create the irregular settlement which leading to failure of construction, illustrated in Figure 1 [5].

The fundamental problem of creep theories is the determination of the stress-strain-time relationship. Because of the complexity of the creep phenomenon and the large number of factors influencing it, several creep theories have been developed to describe creep behaviour in a wide range of real materials. These theories differ in one way in the equations of state correlating stress, strain and time, $\epsilon_t = f(\sigma_t, t)$ or $\sigma_t = f(\epsilon_t, t)$, and in another in the way about how to achieve these equations or how to describe creep phenomena [6].



Fig.1 Illustration of the uneven surface due to creep deformation of subgrade, [5]

Hu studied the effective stress modeling of creep behaviour and presented two main approaches for investigation the creep behavior of soils. The first approach is the rheological modeling approach, which involves combining spring, dashpot, and slider elements in a mathematical analogy that fits the observed soil behavior. The second approach is the phenomenological approach, in which the creep behavior is related to laboratory tests [7].

According to the acting stress, Yao and Fang postulated that the creep strain tensor can be divided into distinct but interdependent, volumetric and deviatoric components. Here, volumetric creep is caused by the constant volumetric stress and deviatoric creep is caused by the constant deviatoric stress [8]. Kosit and Warat investigated the time-dependent response of soils and suggested a simple three-parameter phenomenological equation to describe the relationship between axial strain rate and time of soil samples subjected to a constant deviatoric stress for a wide variety of soils [9].

Han and Zhu developed an alternative creep function that explicitly considers the effects of over-consolidated. It was found that the normalized deviator stress is a unique function of three variables: strain, strain rate, and OCR. They also investigated the effects of over-consolidated based on the relationship adopted to correlate the normalized shear strength of over-consolidated clay and the normalized shear strength of normally consolidated clay [10, 11]. YIN and Li studied the secondary consolidation of soft soil and have proposed the concept of absolute and relative time coordinate system and suggested the use of the absolute time coordinate system in computation of secondary compression. A new method to compute secondary compression was developed based on Bjerrum's theory of e -log p curve and absolute time coordinate system [12, 13]. Li also proposed a model of secondary consolidation which reflects the relationship between time and load. This model, which can be used for both normally consolidated soil and over-consolidated soil, also explained many tested phenomena and engineering problems, such as influences of preloading and unloading on secondary consolidation [14, 15].

This study aims to investigate the creep rate for over consolidation soft clay under plain strain condition through laboratory tests. Based on the consolidation theory combined with the test results evaluating the deformation of soil in the over-consolidation state, and by using the variation of pore water pressure as a predictive parameter and controlling the axial, lateral and volumetric creep strain under static loading condition.

2. RESEARCH SIGNIFICANCE

Based on the plain strain tests results, the deformation rate can be evaluated from the strain of soft clay after consolidation stage. This is an important index for predicting the settlement of soft ground under static loads. Moreover, under drained condition, the study also shows that the variation of pore water pressure is compatible with the axial strain of the soil in the over-consolidated state. Therefore, the measured pore water pressure values can be used to assess the long-term settlement of the soft ground after construction.

3. LABORATORY STUDIES

3.1. Soil Specimen

Undisturbed specimens of soil were sampled from a depth of 4.0 m to 9.0 m, from a soft clay deposit located beneath the embankment of the Shanfen highway. The specimens were taken from a sample of size 15 cm diameter and 25 cm height. A specimen was then cut into a section suitable for size of plane strain creep tests in cuboid shape with height, width and length of 10 cm, 5 cm and 10 cm respectively. The specimen, after removing from the trimming knife, was placed into a split-part mould to keep it in fixed shape and vacuum-saturated in a dedicated system under vacuum pressure of 0.8MPa for at least for 24 hours.

The specimen is confined by a chamber assembled from rigid metal plates and the load is subjected to specimen in both the vertical and lateral directions (i.e., along the Z and X axis respectively), while the strain is restricted in the Y direction (see Figure 2). The soil properties were as follows: density $\rho = 1.52 \sim 1.56 \text{ g/cm}^3$, natural water content $w_n = 61.4 \sim 66.6\%$, plasticity index $I_p = 22 \sim 25\%$, liquidity index $I_L = 1.1 \sim 1.5\%$, initial void ratio $e = 1.65 \sim 1.83$, degree of Saturation $S_r = 96.9 \sim 98\%$, compression factor $\alpha_{0.1-0.2} = 1.61 \sim 1.84 \text{ MPa}^{-1}$, compression modulus $E_s = 1.31 \sim 1.42 \text{ MPa}$, coefficient of consolidation $C_{v100} = 0.448 \times 10^{-3} \sim 0.704 \times 10^{-3} \text{ cm}^2/\text{s}$ and $C_{v200} = 0.645 \times 10^{-3} \sim 0.667 \times 10^{-3} \text{ cm}^2/\text{s}$. All data were determined from tests according to JTG E40-2007 Test Methods of Soils for Highway Engineering.

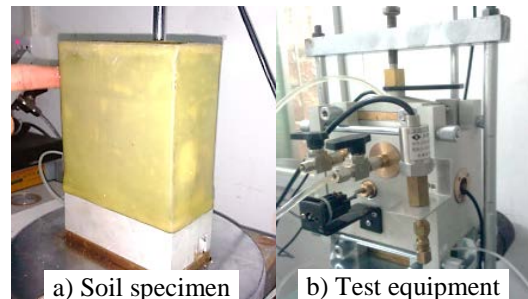


Fig.2 Photos of the test process

3.2. Test Procedure

Plane strain creep test was developed based on the principle of conventional triaxial testing, featuring both the loading system of the former and air pressure controlling system of the latter. Hence, it is possible to apply not only the vertical stress but also the lateral air pressure. The test apparatus was reassembled and calibrated properly to serve the purpose of this research. Figure 3 illustrates a schematic of plane strain test principle.

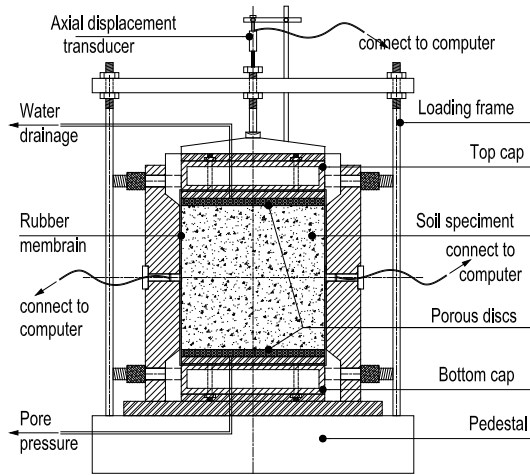


Fig.3 Schematic of test equipment

3.3. Data Acquisition System

In order to measure the change in pore water pressure, strain, lateral pressure, water drainage and magnitude of cyclic load, the transducers are made in the correlative position and connected to the channels display electronic readout unit. The readout unit is further connected, to a Data Acquisition System, which in turn, is connected to the computer. A careful programming of Visual Basic was done to obtain a meaningful data output from the plane strain creep tests both in the form of numbers and step by step graphical presentation to elaborate the changes happening to the sample being tested.

3.4. Loading Scheme

A series of creep tests were carried out by using the plane strain creep apparatus for both normally and over-consolidated clay, in which the principal stress ratio equals K value of 0.5, under the stress control method for the each loading steps. The principal stress ratio, K , is defined as $K = \sigma_x / \sigma_z$, where σ_x and σ_z are the effective lateral and vertical stresses in static load case respectively.

In the initial loading step, the specimens were consolidated under a sustained load ($\sigma_x - \sigma_z$) of (25

- 25) kPa for 24 hours in order to eliminate the differences of various soil specimens, such as the differences in the initial pre-compression, the physical properties and the non-uniform dispersion of the clay particles.

In the next steps, the specimens were subjected to a constant K value of 0.5 with vertical consolidation stresses, σ_z values of 100, 200, 300, 400 kPa for static loading tests. The loading scheme of static test scheme is summarized in Table 1 and shown in Figure 4.

Table 1 Loading scheme of static tests

State	Static Loading (σ_x, σ_z)/kPa	Duration for loading step /days	
Normal consolidation	(25, 25)	Initial	1
	(50, 100)- (100, 200)- (150, 300)- (200, 400)	Creep	7
Over consolidation	(25, 25)	Initial	1
	(50, 100)- (100, 200)- (150, 300)	Consolidation	1
	(25, 25)	Rebound	1
	(50, 100)- (100, 200)- (150, 300)	Creep	7
Over consolidation	(25, 25)	Initial	1
	(50, 100)- (100, 200)- (150, 300)- (200, 400)	Consolidation	1
	(25, 25)	Rebound	1
	(50, 100)- (100, 200)- (150, 300)- (200-400)	Creep	7

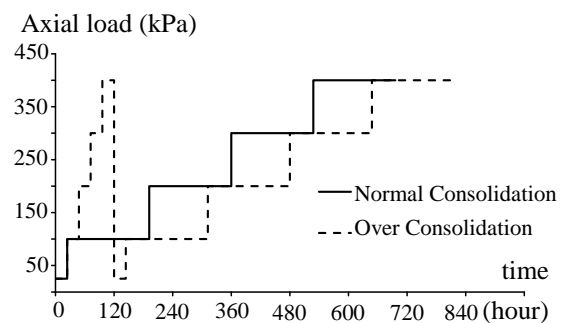


Fig.4 Loading schematic in plane strain tests

4. TEST RESULTS AND ANALYSIS

4.1. Creep Deformations of Saturated Soil

4.1.1 Volumetric creep strain:

Figure 5 shows the relationship between volumetric creep strain, ϵ_v , and elapsed time for soils tested in normally consolidated state. In here,

the maximum values of volumetric creep strain, ε_{vmax} , of 5.1%, 10.2% and 15.7% were obtained for external stress values, (σ_x, σ_z) , of (50, 100) kPa, (100, 200) kPa and (150, 300) kPa, respectively, over the time period of 7 days.

Therefore, it can be concluded that in the normally consolidated state, the ε_{vmax} of soil specimens subjected to static loading increases with the increasing magnitude of external load for the same value of principal stress ratio, K , of 0.5.

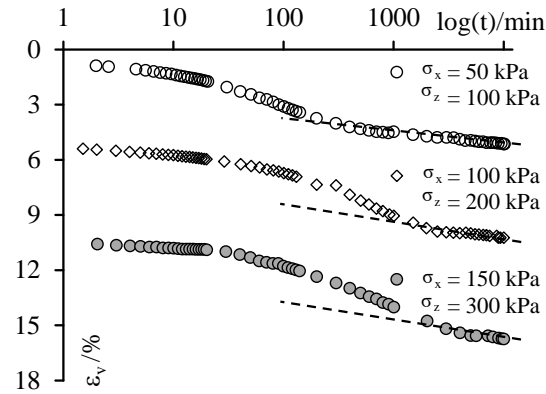


Fig.5 Volumetric creep strain curves

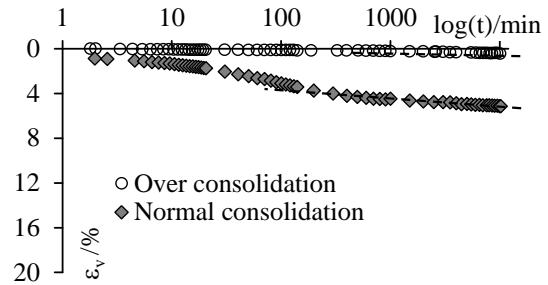
It can be seen that ε_v increases rapidly in the initially period of loading, then tends to a constant value during the creep process. In addition, the slope of the dashed lines shows that the curves are quite parallel. Thus, the rate of change in volumetric creep strain for different loading cases is probably constant during creep and it is independent of the external load level.

Figure 6 (a-d) presents volumetric creep strain histories for various magnitudes of static loading. These curves show that in the overconsolidation state, ε_v increased with the increasing magnitude of external load, but it is much smaller in comparison with that of normally consolidated state at the same value of current loading magnitude. Moreover, it can be observed from the slope of the dashed line that the rate or change of volumetric creep strain decreases rapidly when the soil specimen under static loading changed from the normally to over-consolidated state.

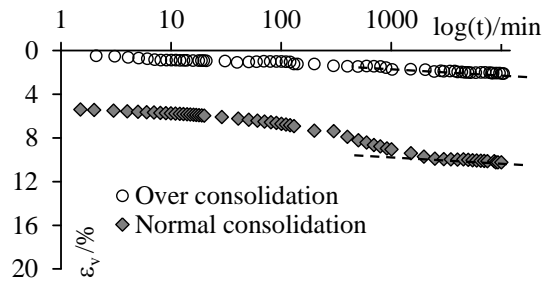
The maximum values of volumetric creep strain, ε_{vmax} , obtained over the time period of 7 days for various values of static loading magnitudes (σ_x, σ_z) , of (50, 100) kPa, (100, 200) kPa, (150, 300) kPa and (200, 400) kPa, respectively are summarized in Table 2. The data shows that for over-consolidated soil sample subjected to static loading, a larger pre-consolidation load value is associated with a significantly reduced volumetric creep strain, the variation decreased from 4.67% to 13.94%.

Table 2 Volumetric creep strain, ε_{vmax} (%)

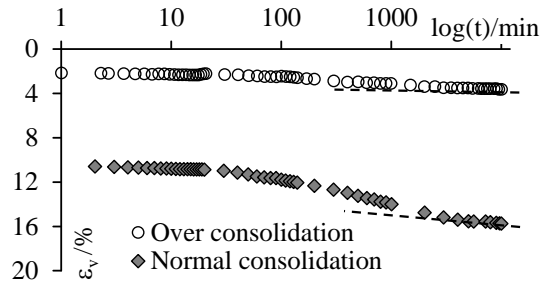
State	Pre-consolidation loading (σ_x, σ_z) _m /kPa	Current loading (σ_x, σ_z) /kPa			
		50, 100	100, 200	150, 300	200, 400
Normally	-	5.1	10.2	15.7	19.9
Over	150, 300	4.01	6.35	8.97	10.1
	200, 400	0.43	2.11	3.64	5.96
$\Delta\varepsilon_{vmax}/\%$		4.67	8.09	12.06	13.94



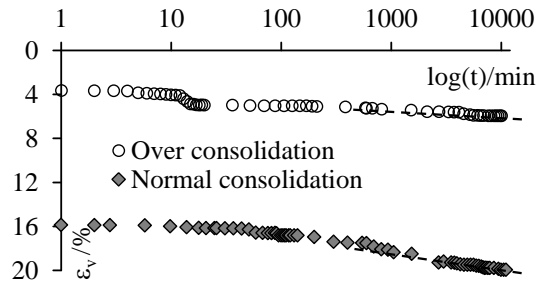
a) $(\sigma_x, \sigma_z) = (50, 100)$ kPa



b) $(\sigma_x, \sigma_z) = (100, 200)$ kPa



c) $(\sigma_x, \sigma_z) = (150, 300)$ kPa



d) $(\sigma_x, \sigma_z) = (200, 400)$ kPa

Fig.6 (a-d) Volumetric creep strain histories for specimen subjected to static loading

4.1.2. Axial creep strain:

Figure 7 displays the axial creep strain versus time results for the static loading tests with the different magnitudes of pre-consolidation loading designated as $(\sigma_x, \sigma_z)_m$. Figure 7a shows the results for $(\sigma_x, \sigma_z)_m = (200, 400)$ kPa, where change in axial creep strain, ε_z , values of 0.23%, 1.10%, 2.15% and 4.09% were obtained for current loading values, (σ_x, σ_z) , of (50, 100) kPa, (150, 300) kPa and (200, 400) kPa, respectively, over the time period of 7 days. Over the same time period, ε_z values of 0.44%, 1.65% and 3.84% , were obtained for (σ_x, σ_z) values of (50, 100) kPa, (100, 150) kPa and (150, 300) kPa respectively for $(\sigma_x, \sigma_z)_m$ value of (150, 300) kPa shown in Figure 7b.

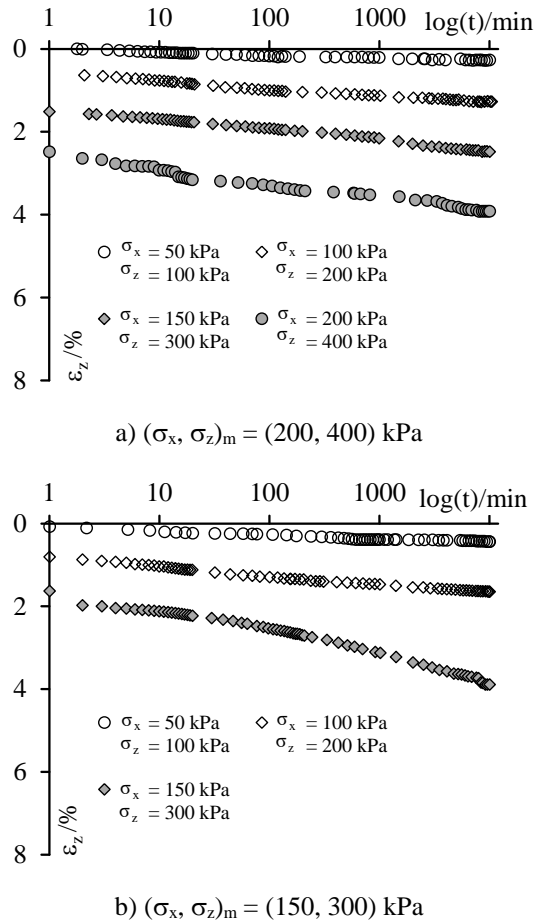


Fig.7 (a-b) Axial creep strain histories for different of pre-consolidation load under static condition

These curves indicate that in the over consolidation state, ε_z increase with increasing magnitude of external load, and it depends on the amplitude of pre-consolidation load, $(\sigma_x, \sigma_z)_m$. The higher pre-consolidation loading, the smaller is the axial creep strain of over-consolidated soil specimen under static loading. Furthermore, all of these curves are rather ramp, which shows that the

axial creep strain varies slowly as be invariable as during total time of tests of 7 days in plane strain condition.

In order to evaluate the effect of the consolidation state on the distribution of axial creep strain, Figure 8 (a-d) is plotted for axial creep strain histories of soil specimen at various static loading levels. The Figure shows that in the over consolidation state, ε_z increased with increasing external load, but the values are much smaller in comparison with those for the case of normally consolidated state at the same values of current loading magnitude.

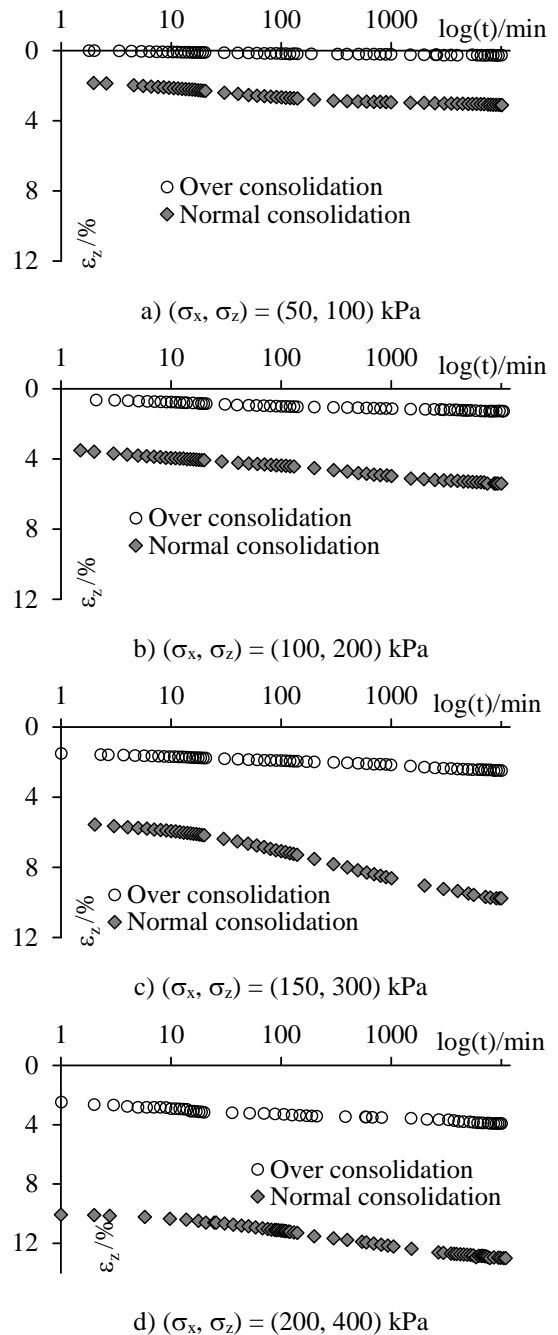


Fig.8 (a-d) Axial creep strain histories

Table 3 below summarizes the maximum value of axial creep strain, $\varepsilon_{z\max}$, for various magnitudes of static loading.

Table 3 Axial creep strain, $\varepsilon_{z\max}$ (%), under static loading

State	Pre-consolidation loading (σ_x, σ_z) _m /kPa	Current loading (σ_x, σ_z) /kPa			
		50, 100	100, 200	150, 300	200, 400
Normally		3.10	5.41	9.77	13.01
Over	150, 300	0.44	1.65	3.84	-
	200, 400	0.26	1.27	2.48	3.92

4.1.3. Lateral creep strain:

Figure 9 and Figure 10 shows the lateral creep strain histories, ε_x , for both normally and over-consolidated test samples subjected to static loading. The curves correspond with lateral strain for different loading levels, and do not include cumulative deformation. It can be seen that the trend of lateral creep strain all load levels are quite similar. In the initial stages of loading, where the elapsed time is less than 80 minutes, test sample tends to develop deformation in lateral expansion direction, value of ε_x less than zero. The lateral strain reduces rapidly to the minimum value, then starts to increase gradually and approaches a certain constant value that is larger than zero in the creep process.

Table 4 Lateral creep strain, ε_x (%), in plane strain tests

Stress (σ_x, σ_z)/kPa	Lateral creep strain, ε_x /%	
	Normal Consolidation	Over Consolidation
50, 100	2.045	0.162
100, 200	2.812	0.673
150, 300	1.141	0.323
200, 400	0.942	0.891

In addition, the lateral creep strain of soil samples in over-consolidated state are smaller than that in normally consolidated state at the same external load level as shown in Table 4. For each loading level in which the principal stress ratio equals K state of 0.5, the soil sample is compressed in shrinkage state, with the magnitude of lateral creep strain not exceeding 3%.

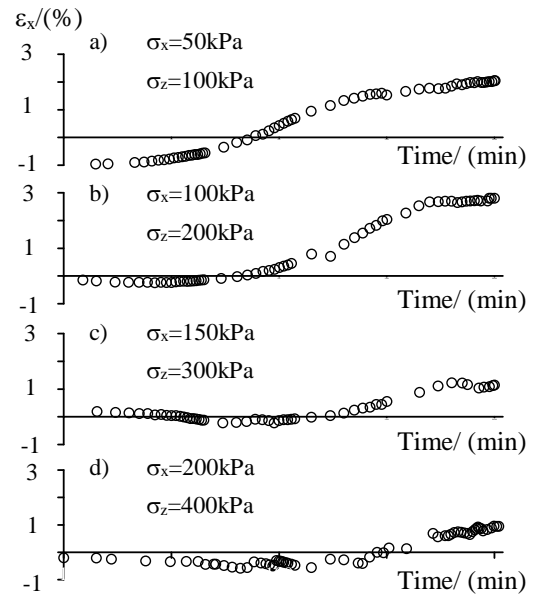


Fig.9 Variation of lateral creep strain under static loading for normal consolidation state

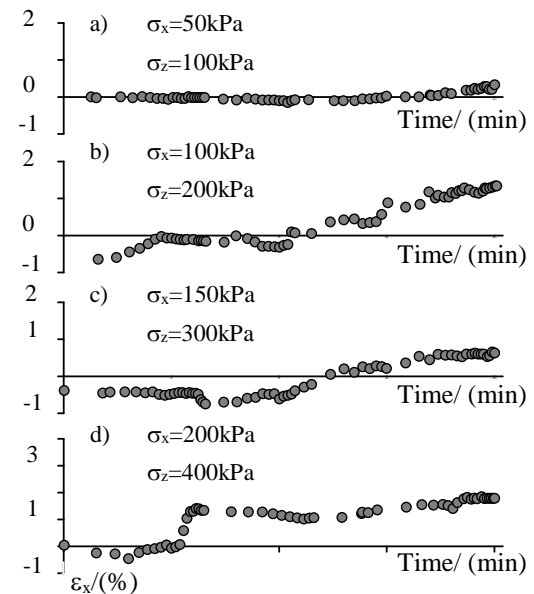


Fig.10 Variation of lateral creep strain under static loading for over consolidation state

The trend of lateral creep strain is consistent with the distribution of excess pore pressure. In the initial period when the external load is applied, the compression of soil sample has tendency to deform by expanding laterally due to the effect of axial loading, σ_z , which is larger than lateral loading, σ_x . Under the effect of external load that is maintained constant during creep process later, the excess pore pressure will be generated and distributed under drainage condition. Both the volumetric and axial strain of soil samples increase rapidly, leading to a decrease in volume of samples. The volumetric strain in here is calculated by the volume of water drained out. The soil particles move closer together,

the void volume of the soil decreases, and this rearrangement make the soil structure become more stable, and the rate of strains decreases gradually. In the creep deformation period, pore pressure gradually reaches a stable equilibrium value of almost zero, the lateral creep strain increases due to σ_x , and the deformation is shrinkage.

4.2. Excess Pore Water Pressure

Figure 11 (a-b) displays the excess pore pressure versus elapsed time curves under the static load condition. It can be seen that the excess pore pressure develops and increases rapidly to reach the peak values as soon as the external loads was applied on the sample, and then decreases gradually to a stable value of zero during creep deformation stage of soil specimen. The peak excess pore pressure and corresponding time are dependent on the magnitude of external loading and consolidation state of soil specimen as shown in Table 6.

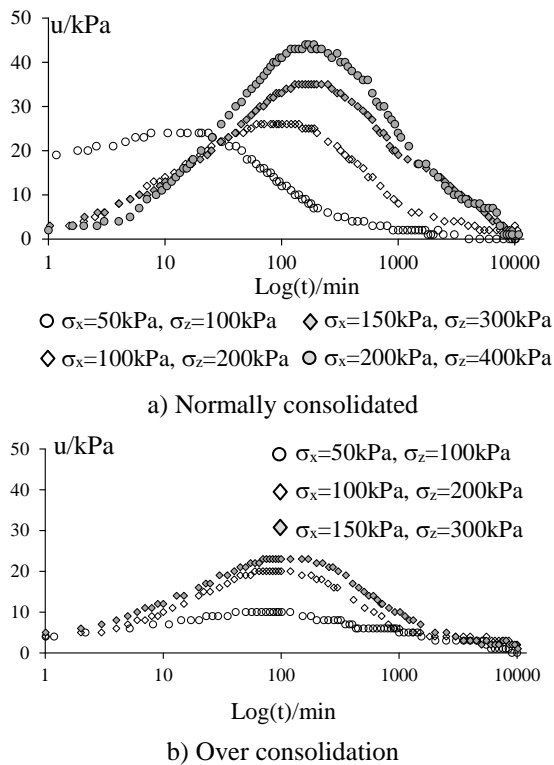


Fig.11 (a-b) Variation of excess pore water pressure due to static loading

Table 5 shows that the peak excess pore pressure, u_{max} , and the time at which it reaches maximum, t_{max} , in both normally and overconsolidation state increase with increasing magnitude of external loading. However, u_{max} for normally consolidated state is much higher in comparison with that for over-consolidated state.

In addition, it can be realized from the t_{max} values and the slope of these curves that the rate of distribution of excess pore pressure is much slower when soil samples changed from the normally to over-consolidated state.

Table 5 Excess pore pressure in plane strain tests

Stress (σ_x, σ_z) /kPa	Normally Consolidation		Over Consolidation (σ_x, σ_z)/kPa			
	u_{max} /kPa	t_{max} /min	(150, 300)		(200, 400)	
			u_{max} /kPa	t_{max} /min	u_{max} /kPa	t_{max} /min
50, 100	24	20	10	41	7	40
100, 200	26	80	20	60	17	55
150, 300	35	130	23	75	20	60
200, 400	44	200	-	-	22	250

Note: u_{max} is the peak value of pore water pressure.

5. CONCLUSIONS

Plane strain creep tests on a soil samples subjected to static loading has been used to investigate the creep behavior of saturated soft clay. This study demonstrates that the deformation behavior of soft clay in the over-consolidated state is equivalent to that in the normally consolidated state, and it should not be neglected in predicting the long-term settlement of structures. This deformation is considered to be a creep (secondary consolidation) of soft clay and can be evaluated by the variation of pore water pressure under the plain strain and drained consolidation.

The following conclusions were obtained from this study: 1) Creep deformation of soft clay depends on the amplitude of pre-consolidation load and the variation of creep strain under static decreases rapidly when the soil changed from the normally to over-consolidated state; 2) Under drained condition the variation of pore water pressure is compatible with the axial creep strain of soft clay in the over-consolidated state. Therefore, the measured pore water pressure values can be used to assess the long-term settlement of the soft ground after construction.

On the other hand, the limitations of the study are restricted to static loading conditions, with the K ratio (is defined as $K = \sigma_x / \sigma_z$) being set at 0.5. A more advanced direction for future research would be to investigate under dynamic loading conditions and consider varying K ratios to assess the deformation variation under changing specific conditions.

6. REFERENCES

- [1] Maslov N.N., Maslov's ideas in modern geomechanics. *Soil Mechanics and Foundation Engineering*, Vol.35, 1998, pp. 173-182.
- [2] Leroueil S., Compressibility of Clays: Fundamental and Practical Aspects. *ASCE Journal of Geotechnical Engineering*, Vol.122, Issue 7, 1996, pp. 534-543.
- [3] Vergote T. A., Leung C. F., and Chian S. C., Modelling creep and swelling after unloading under constant load and relaxation with Bayesian updating. *Géotechnique*, Volume 72 Issue 6, 2022, pp. 496-509.
- [4] Makoto F., Taro U., Junfeng T., and Shanging T., Verify the prediction of slope failure by soil creep with laboratory experiments. *International Journal of GEOMATE*, Vol.23, Issue 98, 2022, pp. 164-170.
- [5] Lei H. Y., Liu M., Jiang Y., and Sun X. F., Deformation of Tianjin soft clay and corresponding micromechanism under cyclic loading. *Canadian Geotechnical Journal*, Vol.57, Issue 12, 2020, pp. 1893-1902.
- [6] Gu C., Wang Y. Z., Cai Y. Q., and Wang J., Deformation characteristics of saturated clay in three-dimensional cyclic stress state. *Canadian Geotechnical Journal*, Vol.56, Issue 12, 2019, pp. 1789-1802.
- [7] Hu Y. Y., Yang P., and Yu Q. Z., Time effect of secondary consolidation coefficient of over-consolidated soil. *China Journal of Highway and Transport*, Vol. 29, Issue 9, 2016, pp. 29-37.
- [8] Yao Y. P., and Fang Y. F., Negative creep of soils. *Canadian Geotechnical Journal*, Vol. 57, Issue 1, 2020, pp. 1-16.
- [9] Kosit J., and Warat K., Effects of temperature on strength and time-dependent deformation behaviours of hostun sand under shear. *International Journal of GEOMATE*, Vol.24, Issue 10, 2023, pp. 84-93.
- [10] Han J., Yin Z. Y., Dano C., and Hicher P. Y., Cyclic and creep combination effects on the long-term undrained behavior of overconsolidated clay. *Acta Geotechnica*, Vol.16, Issue 4, 2021, pp. 1027-1041.
- [11] Zhu H. H., Zhang C. C., Mei G. X., Shi B., and Gao L., Prediction of one-dimensional compression behavior of Nansha clay using fractional derivatives. *Marine Georesources & Geotechnology*, Vol.35, Issue 5, 2016, pp. 688-697.
- [12] Yin Z. Z., Zhang H. B., Zhu J. G., Li G. W., Secondary consolidation of soft soils. *Chinese Journal of Geotechnical Engineering*, Vol.25, Issue 5, 2003, pp. 521-526.
- [13] Li G. W., Zhou Y., Ruan Y. S., Huang K., and Yin J. H., Plane strain tests on creep characteristics of over-consolidated clay. *Chinese Journal of Geotechnical Engineering*, Vol.36, Issue 6, 2014, pp. 1028-1035.
- [14] Li G. W., Huang K., Ruan Y. S., Li X., and Yin J. H. The effect of principal stress ratio on creep behavior of over-consolidated clay under plane strain. *Chinese Journal of Rock Mechanics and Engineering*, Vol. 34, Issue 12, 2015, pp. 2550-2558.
- [15] Li G. W., Li X., Ruan Y. S., Hou Y. Z., and Yin J. H., Creep model of over-consolidated soft clay under plane strain. *Chinese Journal of Rock Mechanics and Engineering*, Vol.35, Issue 11, 2016, pp. 2307-2315.

Copyright © Int. J. of GEOMATE All rights reserved, including making copies, unless permission is obtained from the copyright proprietors.
